

Structural, electronic properties of ScMn₂ alloy and its hydride from first-principles calculations

DU XIAOMING*, MA PING^a, WU ERDONG^a

School of Materials Science and Engineering, Shenyang Ligong University, Shenyang 110159, PR China;

Institute of Metal Research, Chinese Academy of Sciences, Shenyang 110016, PR China

Structural, energetic and electronic properties of ScMn₂ alloy and its hydride ScMn₂H_{1.5} were investigated by means of first-principles calculations within a framework of the density function theory. The obtained structural parameters were close to the available experimental results. The cohesive energies and enthalpies of formation for ScMn₂ and ScMn₂H_{1.5} were calculated to analyze the stability. The calculated results shown that the stability of the hydride ScMn₂H_{1.5} was higher than that of ScMn₂ alloy. The density of states, the charge density distribution and Mulliken charge populations were investigated in order to get insight into the underlying mechanism for structural stability and electronic bonding nature of ScMn₂ and ScMn₂H_{1.5}.

(Received April 23, 2013; accepted July 11, 2013)

Keywords: ScMn₂ alloy, Hydride, Electronic structure, First-principles calculations

1. Introduction

AB₂ Laves phases intermetallics are composed of two different metallic atoms A and B with the different atomic radii; usually $r_A:r_B \approx 1.2:1$. The Laves phases crystallize in three structure types, which are named after the representatives hexagonal C14 (MgZn₂ type), cubic C15 (MgCu₂ type), and hexagonal C36 (MgNi₂ type) [1]. The most prominent application for Laves phases intermetallics is the utilization of Laves phases as hydrogen storage materials especially in nickel–metal hydride batteries on the basis of the Laves phase Zr(V,Mn,Ni)₂ [2-4]. Most of hydrogen storage alloys with Laves phase belong to C14 or C15-type structures, and only a few C36-type compounds can absorb hydrogen.

Recently, The Sc-based Laves phase alloys (ScMn₂, ScMnCr, ScFe₂, ScCo₂, ScNi₂, etc.) have attracted extensive attention on hydrogen storage properties due to their fast kinetics, high storage capacity and good structural stability. Li et al [5-7] have reported the experimental results of the crystal structures and hydrogen storage properties for ScMnCr and ScMn₂ alloys. They pointed out that Sc-based alloys with Cr-Mn as common component exhibit extraordinary catalytic effect on hydrogen dissociation and absorption. Yoshida et al [8] studied the hydrogen absorbing properties of ScM₂ (M = Fe, Co and Ni) Laves phase alloys and estimated the enthalpies of the hydride formation. However, the results of theoretical investigation, such as the change of electronic states in hydrogenation process, the transfer of the charges, the bonding nature and bonding modes between hydrogen atoms and alloying elements and the

interaction mechanism between hydride-generation and non-hydride-generation elements for ScMn₂-H₂ system have not been reported so far to our knowledge.

In the studies described in this paper, the crystal structures and electronic properties of ScMn₂ alloys and its hydride are investigated by using the pseudopotential plane-wave method based on density functional theory. The enthalpies of formation, cohesive energy of the alloy and its hydride are estimated, and the bonding nature of hydrogen atoms and alloying elements in the hydrides of ScMn₂ alloys is described.

2. Method and models

All calculations were performed using density functional theory (DFT) as implemented in the Quantum-ESPRESSO [9]. It uses a plane-wave basis set for the expansion of the single-particle Kohn–Sham wave functions, and pseudopotentials to describe the computationally expensive electron–iron interaction, in which the exchange–correlation energy by the generalized gradient approximation (GGA) [10] is adopted for all elements in our models by adopting the Perdew–Burke–Ernzerhof [11] parameters. Ultrasoft pseudopotentials [12] represented in reciprocal space were used. For ScMn₂ alloys, we used a 6×6×4 Monkhorst–Pack [13] *k*-point mesh for sampling Brillouin zone. For the hydride ScMn₂H_{1.5}, *k*-point sampling was performed on a 5×5×4 grid. A Gamma centered 18×18×12 mesh was used for cubic metals Sc and Mn. Convergence with respect to the *k*-point sampling for the Brillouin zone

(BZ) integration was tested independently on the two compounds using regular meshes of increasing density. Tests indicated that the total energy converges to 1 meV/atom. The valence electronic configurations were taken to be $3s^23p^6 3d^1 4s^2$ for Sc, $3s^23p^63d^54s^24p^0$ for Mn and $1s^1$ for H. The cut-off energy of atomic wave functions (PWs) was set at 310 eV for all the calculations. For all structures the lattice parameters, the volume and the atom positions were allowed to relax simultaneously. The relaxations of cell geometry and atomic positions were carried out using a conjugate gradient algorithm until the Hellman–Feynman force on each of the unconstrained atoms was less than $0.01\text{eV}/\text{\AA}$. The self-consistent calculations were considered to be converged when the difference in the total energy of the crystal did not exceed 10^{-6} eV at consecutive steps. After the structures are optimized, the total energies are recalculated self-consistently with the tetrahedron method [14]. The latter technique is also used to calculate the electronic density of states (DOS).

ScMn_2 crystallizes in C14-type Laves phase structure with symmetry $P6_3/mmc$ [15], and the unit cell of ScMn_2 contains 4 Sc atoms and 8 Mn atoms, as shown in Fig. 1 (a). Li et al. [7] charged the alloy sample with hydrogen gas, the composition of the formed hydride was found to correspond to ~ 3.6 atoms of H per formula unit (referred to as $\text{ScMn}_2\text{H}_{3.6}$). And the hydrogen storage capacity of 2.1 wt.% can be achieved [7]. The XRD investigation results of $\text{ScMn}_2\text{H}_{3.6}$ indicated that the hydrogenation of the ScMn_2 alloy did not alter the matrix lattice structure [7]. The structural type obtained from hydride $\text{ScMn}_2\text{H}_{3.6}$ was very similar to that of the alloy, with nearly ideal values for the close-packed C14 structure. In the AB_2 Laves-phases all the interstitial sites are tetrahedral and can be of A_2B_2 , AB_3 and B_4 types. At low hydrogen contents, hydrogen atoms preferentially occupies A_2B_2 sites, which in the hexagonal C14 can be distinguished in four non-equivalent types ($6h_1$, $6h_2$, $12k$ and $24l$). The neutron diffraction studies of Sun et al. on the deuterated C14 compound $\text{Zr}_{0.9}\text{Ti}_{0.1}\text{MnCr}$ showed that hydrogen atoms in ternary hydrides, based on the C14-type, occupy interstitial tetrahedral-like A_2B_2 interstitial sites [16,17]. And for the saturated deuteride $\text{Zr}_{0.9}\text{Ti}_{0.1}\text{MnCrD}_{3.5}$, the occupancies of D atoms in the $6h_1$ and $12k$ sites are higher in comparison with that of the $6h_2$ and $24l$ sites. In the present work, calculations were done with the assumption that hydrogen is located in $6h_1$ site, which corresponded to ~ 1.5 atoms of H per formula unit (referred to as $\text{ScMn}_2\text{H}_{1.5}$). The structural model of the hydride $\text{ScMn}_2\text{H}_{1.5}$ is shown in Fig. 1 (b).

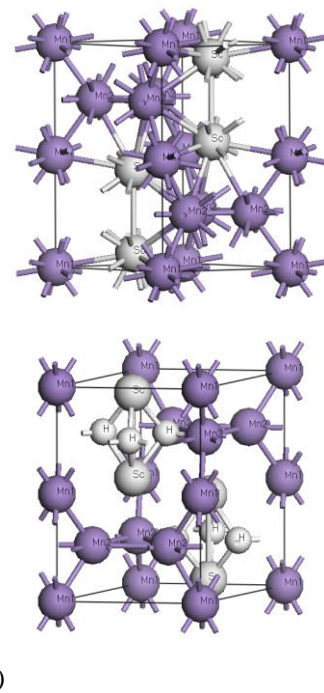


Fig. 1. Crystal structures of ScMn_2 (a) and $\text{ScMn}_2\text{H}_{1.5}$ (b).

3. Results and discussion

3.1 Crystal structure

Starting from the crystal structures shown in Fig. 1, the structural optimization was first performed by full relaxation of cells shape and atomic positions. The atomic positions in the unit cells and lattice constants for ScMn_2 and $\text{ScMn}_2\text{H}_{1.5}$ are given in Tables 1 and 2, respectively. It is found that there are almost no changes in the space group structure of the ScMn_2 phase, and in the metal atom positions in the unit cell with and without hydrogenation. And the calculated metal atom positions for ScMn_2 are in good agreement with experimental values [7,17]. However, hydrogen atom has considerably less deviation from the ideal position of $6h_1$ site. This is likely to be attributed to the influence of the other three interstices which have been ignored in this work. Seen from Table 2, the present lattice constants a and c of ScMn_2 are appreciably less than the experimental values reported in Ref. [7] and the maximum error of the lattice constants calculated here relative to the experimental results is about 1.95 %. However, the unit cell axis c/a ratio (1.641 for ScMn_2) derived by calculation are the same as the experimental values of c/a ratio. Moreover, the lattice constants of the hydride $\text{ScMn}_2\text{H}_{1.5}$, $a = 5.123 \text{ \AA}$ and $c = 8.271 \text{ \AA}$, are smaller than that of the saturated hydride $\text{ScMn}_2\text{H}_{3.6}$ ($a = 5.472 \text{ \AA}$ and $c = 8.908 \text{ \AA}$ [7]). It is known that in a metal–hydrogen system the dissolved hydrogen expands the crystal lattice of the host lattice, and the Sc–Mn–H system is no exception. The lattice expansion is an important measure of hydrogen absorption in the metals. The typical relative volume

expansions due to the solution of one hydrogen atom per metal atom are of the order of 20%. The volume of the hydride ScMn₂H_{1.5} increases by 10.1% compared to that of the alloy (see Table 2). Li et al. [7] reported the value of the increased volume of the saturated hydride ScMn₂H_{3.6}

by 27.7% compared to that of the alloy. The reason is that the small amounts of hydrogen atoms are in 6h₁ interstice, but the 6h₂, 12k and 24l sites are empty for the hydride ScMn₂H_{1.5} with low hydrogen content.

Table 1. Atom positions in the unit cells of ScMn₂ and ScMn₂H_{1.5}.

	Atom	Wyckoff site		Position		
				x	y	z
ScMn ₂	Mn1	2a	Relaxed	0	0	0
			Expt. ^a	0	0	0
	Sc	4f	Relaxed	0.333	0.667	0.437
			Expt. ^a	0.333	0.667	0.436
	Mn2	6h	Relaxed	0.829	0.660	0.250
			Expt. ^a	0.829	0.660	0.250
ScMn ₂ H _{1.5}	Mn1	2a	Relaxed	0	0	0
			Expt. ^a	0	0	0
	Sc	4f	Relaxed	0.333	0.667	0.437
			Expt. ^a	0.333	0.667	0.436
	Mn2	6h	Relaxed	0.843	0.686	0.250
			Expt. ^a	0.835	0.670	0.250
	H	6h ₁	Relaxed	0.479	0.958	0.250
			Expt. ^b	0.462	0.924	0.250

^a From Ref. [7], ^b from Ref. [17].

Table 2. Results for ScMn₂ and ScMn₂H_{1.5} including equilibrium lattice constants, total energy E_{tot} , formation enthalpy ΔH and cohesive energy E_{coh} .

Materials	Lattice parameter (Å)		Space group	Volume (Å ³)	Total energy E_{tot} (eV/f. u.)	ΔH (eV·atom ⁻¹)	E_{coh} (eV·atom ⁻¹)
	a	c					
ScMn ₂	4.934 (5.032) ^[7]	8.096 (8.253) ^[7]	<i>P6₃/mmc</i>	170.711	-10350.771	-0.284	-4.629
ScMn ₂ H _{1.5}	5.123	8.271	<i>P6₃/mmc</i>	187.996	-10435.910	-0.659	-5.670

3.2 Formation enthalpy and cohesive energy

To estimate the stability of ScMn₂ and ScMn₂H_{1.5} phase the formation enthalpies of two unit cells were calculated. The formation enthalpy (ΔH) of per atom of ScMn₂ and ScMn₂H_{1.5} phases were calculated [18,19]:

$$\Delta H(\text{ScMn}_2) = \frac{1}{12} [E_{\text{tot}}(\text{ScMn}_2) - 4E_{\text{tot}}(\text{Sc})_{\text{solid}} - 8E_{\text{tot}}(\text{Mn})] \quad (1)$$

$$\Delta H(\text{ScMn}_2\text{H}_{1.5}) = \frac{1}{3} [E_{\text{tot}}(\text{ScMn}_2\text{H}_{1.5}) - 8E_{\text{tot}}(\text{Mn})_{\text{solid}} - 4E_{\text{tot}}(\text{Sc})_{\text{solid}} - 3E_{\text{tot}}(\text{H}_2)] \quad (2)$$

where $E_{\text{tot}}(\text{ScMn}_2)$ and $E_{\text{tot}}(\text{ScMn}_2\text{H}_{1.5})$ are the total energy of ScMn₂ and ScMn₂H_{1.5} cell unit, as shown in Table 2. $E_{\text{tot}}(\text{Sc})_{\text{solid}}$ and $E_{\text{tot}}(\text{Mn})_{\text{solid}}$ are the single atomic energy in pure solid states Sc and Mn.

$E_{\text{tot}}(\text{H}_2)$ is the total energy of hydrogen molecule, which was calculated as 31.5652 eV using the von Barth-Hedin exchange correlation potential [20]. In the present work, we calculate the single atomic energy by the following

method: at first, the energy of a pure metal crystal in the solid state was calculated, then the energy was divided by the number of atoms involved in the crystal, and this result is the energy of a single atom in the pure metal. The calculated energies of Sc and Mn atoms for our considered systems were -1277.896 eV and -654.472 eV, respectively. The calculated formation enthalpies of ScMn₂ and ScMn₂H_{1.5} phases are also listed in Table 2. It was found that the formation enthalpy of ScMn₂H_{1.5} phase is much more negative than that of ScMn₂. The lower the formation enthalpy is, the more stable the crystal structure is. This suggests clearly that the hydride is very stable relative to the elemental constituents. The present formation enthalpy of ScMn₂ phases is -0.284 eV·atom⁻¹ (27.4 kJ·mol⁻¹), which is close to the values -26.1 kJ·mol⁻¹ [21] and 30 kJ·mol⁻¹ [8] measured experimentally. For ScMn₂H_{1.5} phase, the value of the formation enthalpy obtained experimentally by Shilov et al. [22], Griessen et al. [23] and Li et al. [7] was 63.0 kJ·mol⁻¹, 40.2 kJ·mol⁻¹ and -45.2 kJ·mol⁻¹, respectively. Hence, the value of the calculated formation enthalpy of ScMn₂H_{1.5} phase (0.659 eV·atom⁻¹ equals 63.6 kJ·mol⁻¹) in this work is close to the result obtained by Shilov et al. [22].

The cohesive energy (E_{coh}) is defined as the difference between the total energy of crystal and the total energy of the isolated atoms.

$$E_{\text{coh}} = E_{\text{tot}}(\text{solid}) - \sum_i E_i(\text{isolated}) \quad (3)$$

where $E_{\text{tot}}(\text{solid})$ is the total energy of the compounds at equilibrium lattice constant, and $E_i(\text{solid})$ is the total energies of the isolated constituent atoms at infinite separation. In this case, the cohesive energy of the ScMn₂ and ScMn₂H_{1.5} cell unit per atom was calculated using the following expression [19], respectively.

$$E_{\text{coh}}(\text{ScMn}_2) = \frac{1}{12} [E_{\text{tot}}(\text{ScMn}_2) - 4E_{\text{Sc}}(\text{isolated}) - 8E_{\text{Mn}}(\text{isolated})] \quad (4)$$

$$E_{\text{coh}}(\text{ScMn}_2\text{H}_{1.5}) = \frac{1}{18} [E_{\text{tot}}(\text{ScMn}_2\text{H}_{1.5}) - 4E_{\text{Sc}}(\text{isolated}) - 8E_{\text{Mn}}(\text{isolated}) - 6E_{\text{H}}(\text{isolated})] \quad (5)$$

In order to obtain an accurate value for the cohesive energy, the energy calculations for both isolated atom and the crystal must be performed at the same level of accuracy. The energy of an isolated atom has been calculated using a cubic supercell (irrespective of crystal structure of the corresponding solid) with large lattice parameter of 10 \AA so that the inter atomic interaction is

negligible. The calculated energies of isolated atoms Sc, Mn and H are -1273.4121 , -650.1974 and -1.10351 eV·atom⁻¹, respectively. According to Eqs. (4) and (5), the obtained cohesive energies of ScMn₂ and ScMn₂H_{1.5} phases are -4.629 and -5.670 eV·atom⁻¹, as shown in Table 2. It is found that the cohesive energy of the hydride phase increases when ScMn₂ alloy absorbs hydrogen. In general, the cohesive intensity and structural stability of the crystal are correlated with its cohesive energy [24] being defined as either the energy needed to form the crystal from free atoms or the work needed to decompose the crystal into isolated atoms. The larger the cohesive energy, the more stable is the corresponding crystal structure. The results have indicated that ScMn₂H_{1.5} is more stable than ScMn₂.

3.3 Electronic structure

In order to investigate intrinsic mechanism for structural stability and electronic bonding nature, the density of states (DOS), the charge density distribution and Mulliken charge populations for ScMn₂ and ScMn₂H_{1.5} phases were calculated. Fig. 2 shows the total densities of states (TDOS) and partial densities of states (PDOS) for ScMn₂ and ScMn₂H_{1.5} phases, in which Fermi level was set to zero. The value of the total DOS at Fermi level was 13.74 and 21.42 states/eV for ScMn₂ and ScMn₂H_{1.5}, respectively, which indicated the metallic property.

As shown in Fig. 2 (a), the bonding peaks 1, 2 and 3 located at the energy range from -5.0 eV to -3.0 eV on TDOS plot for ScMn₂ alloy originated from the contribution of the bonding electron numbers of Sc(3s), Mn1(4s) and Mn2(4s) orbitals. The other bonding peaks (including the bonding peaks 4, 5, 6, 7, 8 and 9) located at the energy range from -3.0 eV to 2.5 eV on TDOS plot for ScMn₂ alloy mainly originated from the contribution of the bonding electron numbers of Sc(3d), Mn1(3d) and Mn2(3d) orbitals. Moreover, the Sc(3p), Mn1(4p) and Mn2(4p) states also had a little contribution to above bonding peaks. This indicates that the interactions between Mn atom and Sc atom were derived from the hybridization between Sc(3d) states and Mn(3d) states. The conclusion was consistent with the result reported by Wu et al. [25].

However, the DOSs of ScMn₂H_{1.5} are distinctly different from those of ScMn₂, as shown in Fig. 2(b). Comparing DOSs of ScMn₂H_{1.5} with ScMn₂, it is found that ScMn₂H_{1.5} had the following characteristics: (i) the formation mechanism of peaks 4, 5, 6, 7, 8 and 9 located at the energy range from -3.0 eV to 2.5 eV on TDOS plot for ScMn₂H_{1.5} was the same as ScMn₂ alloy, whereas the height of peak 5 decreased. The main reason was that the contribution of Mn1(3d) orbital electrons to peak 5 weakened upon hydrogenation of ScMn₂ alloy. (ii) The bonding peaks 1, 2 and 3 markedly rose and the new bonding peaks 10 and 11 appeared, which resulted from the contribution of the bonding electron numbers of Sc(3d), Mn2(3d) and H(1s) orbitals. (iii) The density of states for

Sc(3s) and (3p) orbitals had almost no change with and without the hydrogenation of ScMn₂ alloy, whereas the density of state for Sc(3d) orbitals changed obviously. The bonding peaks appeared in the energy range from -8.0 to -5.5 eV, which were formed by the overlap of the H(1s) orbital and the Sc(3d) orbital. Moreover, for the energy range from -7.0 to -5.5 eV, the degree of overlap of the electron orbit for the H(1s) and the Mn2(3d) is higher than that for the H(1s) and the Sc(3d). This shows that the bond strength of H-Mn2 is larger than that of H-Sc.

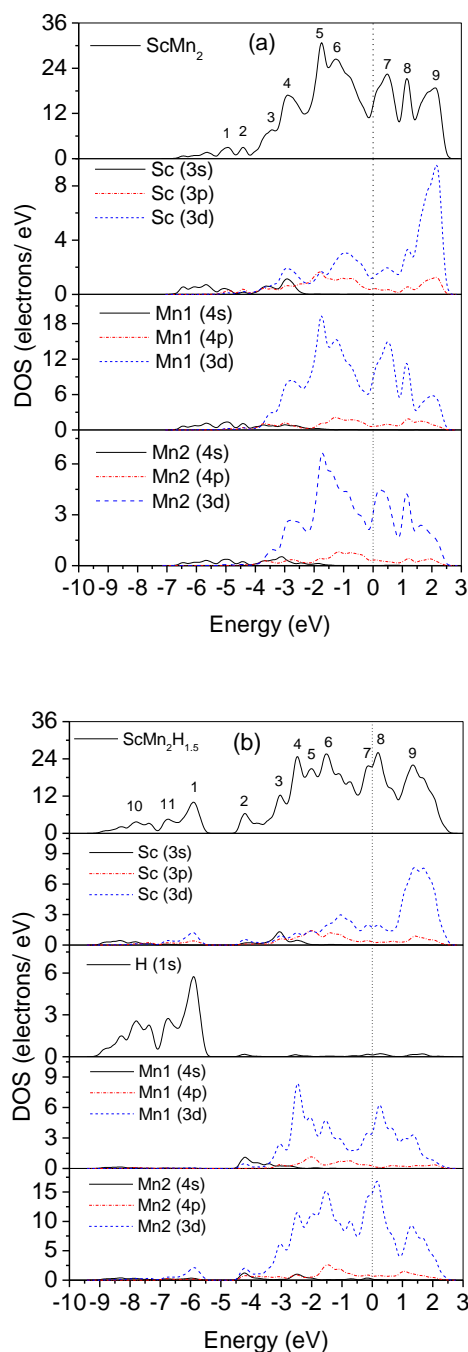


Fig. 2. Total and partial density of states of ScMn₂ (a) and ScMn₂H_{1.5} (b), and Fermi level was set at zero energy and marked by the vertical dot line.

As also shown in Fig. 2 (a) and (b), the density of state for Mn2(4s) and (4p) orbitals had almost no change with and without the hydrogenation of ScMn₂ alloy, whereas the number of electron occupancies of Mn2(3d) orbitals increased obviously. The contribution of Mn2(3d) orbital electrons to the bonding peaks in the energy range from -7.0 to -5.5 eV augmented evidently. And the degree of overlap of the electron orbit for the H(1s) and the Mn2(3d) is very high, suggesting the contribution of the orbital electrons of Mn2(3d) to the bonding in the energy range is stronger than that of other orbital electrons. It is indicated that the interactions between H atom and Mn2 atom were derived from the interactions between Mn2(3d) and H(1s) orbital electrons.

Fig. 3 shows the comparison of Mn2 (3d) electron densities of states in ScMn₂ and ScMn₂H_{1.5}. The peak e on the DOS plot of Mn2(3d) orbitals in ScMn₂H_{1.5} shifted from non-bonding region to Fermi level. At the same time, the contribution of the electron densities of states of Mn2(3d) to the bonding region in the energy range from -8.0 to 5.5 eV increased markedly. The two factors both improve the stability of ScMn₂H_{1.5} phase.

To visualize the nature of the bond character and to explain the charge transfer and the bonding properties of the ScMn₂ and ScMn₂H_{1.5} compounds, we have investigated change of the charge density distribution with and without the hydrogenation of ScMn₂ alloy. Fig. 4 shows the charge-density contours in the (113) plane for ScMn₂ alloy (Fig. 4(a)), as well as in the (013) plane for ScMn₂H_{1.5}

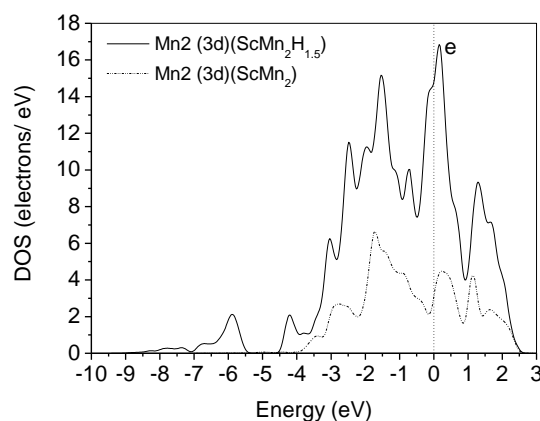


Fig. 3. Comparison of Mn2 (3d) electron densities of states in ScMn₂ and ScMn₂H_{1.5}.

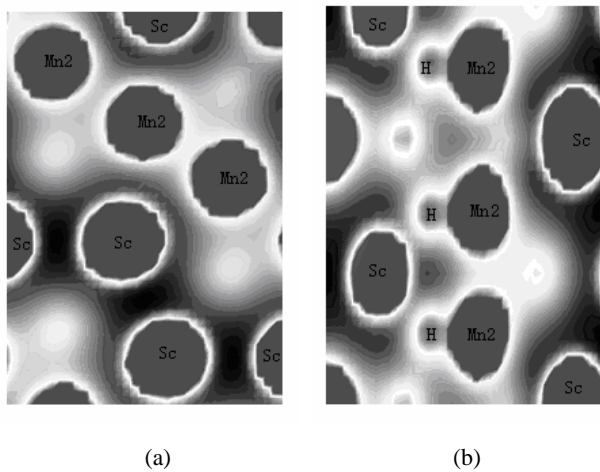


Fig. 4. Contour map of the electron density on the $(\bar{1}\bar{1}1)$ plane for ScMn_2 (a) and the (011) plane for $\text{ScMn}_2\text{H}_{1.5}$ (b).

(Fig. 4(b)). It is found that the interactions between Mn2 and Mn2 atom are stronger than that between Sc and Mn2 atom in the tetrahedron of ScMn_2 (Fig. 4(a)). From the view of the formation enthalpy of the hydrides formed by the elements, hydrogen absorbing alloys are consist of the hydride-generation metals A (Ti, Sc, Zr, Mg and La etc.) with endothermic reaction property during hydrogenation and the non-hydride-generation metals B (Cr, Mn, Fe, Co and Ni etc.) with exothermic reaction property during hydrogenation, such as ScMn_2 , ZrMn_2 , Mg_2Ni . In general, the A metals form easily hydrides (TiH_2 , ScH_2 , ZrH_2 , and MgH_2 etc.), whereas the B metals

are helpful to accelerating hydrogenation process. However, the interactions between H and Mn2 atom are stronger than that between H and Sc atom in $\text{ScMn}_2\text{H}_{1.5}$, as shown in Fig. 4 (b). And the interactions between Mn2 and Mn2 atom are weaker than that between Sc and H atom in $\text{ScMn}_2\text{H}_{1.5}$ (Fig. 4(b)). This trend also were observed in some hydrogen absorbing alloys, such as LaNi_5 [26], Mg_2Ni [27] and TiFe [28]. Moreover, the interactions between Mn2 and Mn2 atom in $\text{ScMn}_2\text{H}_{1.5}$ were weaker than that in ScMn_2 (Fig. 4(a) and (b)).

Table 3 shows the charge populations and average charge populations per unit bond length between two atoms in ScMn_2 alloy and the hydride $\text{ScMn}_2\text{H}_{1.5}$. It is found that there are the chemical bonds between Mn2 and Mn2, Mn2 and Mn1, Mn2 and Sc atoms in ScMn_2 alloy. The charge populations and average charge populations per unit bond length of Mn2-Mn2 are largest of three atom pairs. This indicates that the interaction of Mn2-Mn2 atom pair is stronger than that Sc-Mn2 and Mn2-Mn1 atom pair in ScMn_2 alloy. It is consistent with the results from the charge density distribution (Fig. 4 (a)). After the hydrogenation of ScMn_2 alloy, the bond length of Mn1-Mn2 and Sc-Mn2 both decreased except for Mn2-Mn2 bond, which resulted in improvement of the stability of $\text{ScMn}_2\text{H}_{1.5}$ phase. The increase of the bond length of Mn2-Mn2 resulted from the expanding of the crystal lattice of $\text{ScMn}_2\text{H}_{1.5}$. Thus, the charge populations on Mn2-Mn2 bond reduced. The bond strength of Mn2-Mn2 became weak accordingly, which were weaker than that of H-Mn2 and H-Sc.

Table 3. Charge populations between two atoms in ScMn_2 alloy and $\text{ScMn}_2\text{H}_{1.5}$.

Compounds	Bond	Charge population	Bond length, \AA	Average charge population per unit bond length, \AA^{-1}
ScMn_2	Mn2-Mn2	0.23	2.40705	0.096
	Mn2-Mn1	0.06	2.49515	0.024
	Sc-Mn2	0.14	2.89708	0.048
$\text{ScMn}_2\text{H}_{1.5}$	Mn2-Mn2	0.03	2.47084	0.012
	Mn2-Mn1	0.09	2.42824	0.037
	Sc-Mn2	0.02	2.86886	0.007
	Sc-H	0.07	2.04589	0.034
	Mn2-H	0.09	1.66107	0.054

4. Conclusions

In the present study, we performed the first-principles calculation of energetic, structural and electronic properties of ScMn_2 alloy and its hydride $\text{ScMn}_2\text{H}_{1.5}$ using a basis of a plane-wave pseudo-potential method within a framework of the density function theory. The optimized cell parameters and atomic positions are close to the

existing experimental results. The obtained cohesive energies and enthalpies of formation revealed that ScMn_2 alloy and $\text{ScMn}_2\text{H}_{1.5}$ are energetically favorable, and the stability of the hydride $\text{ScMn}_2\text{H}_{1.5}$ is higher than that of ScMn_2 alloy. The analysis of the density of states, charge density and Mulliken charge population indicates that the interactions between Mn2 and Mn2 atom are stronger than that between Sc and Mn2 atom in the ScMn_2 alloy. Upon

hydrogenation of ScMn₂ alloy, the bond strength of Mn₂-Mn₂ becomes obviously weak, and the interactions between H and Mn₂ atom are stronger than that between H and Sc atom in ScMn₂H_{1.5}. The results can provide helpful guidance for improving hydrogen storage properties of the Sc-based Laves phase alloys.

Acknowledgement

We gratefully acknowledge the financial support from the program for Liaoning Excellent Talents in University (LNET), China (LJQ2012016).

References

- [1] Y. Kitano, M. Takata, Y. Komura, *J. Microsc.* **142**, 181 (1986).
- [2] L. Schlapbach, A. Züttel, *Nature* **414**, 353 (2001).
- [3] Y. L. Du, X. G. Yang, Q. A. Zhang, Y. Q. Lei, M. S. Zhang, *Int. J. Hydrogen Energy* **26**, 333 (2001).
- [4] J. M. Joubert, D. Sun, M. Latroche, A. Percheron-Guegan, *J. Alloys Compd.* **253-254**, 564 (1997).
- [5] W. H. Li, E. D. Wu, *J. Alloys Compd.* **511**, 169 (2012).
- [6] E. D. Wu, W. H. Li, J. Li, *Int. J. Hydrogen Energy* **37**, 1509 (2012).
- [7] W. H. Li, B. H. Tian, P. Ma, E. D. Wu, *Acta Metall. Sin.* **48**, 822 (2012).
- [8] M. Yoshida, E. Akiba, *J. Alloys Compd.* **226**, 75 (1995).
- [9] <http://www.quantum-espresso.org/>.
- [10] J. P. Perdew, J. A. Chevary, S. H. Vosko, K. A. Jackson, M. R. Pederson, D. J. Shingh, C. Fiolhais, *Phys. Rev. B* **46**, 6671(1992).
- [11] J. P. Perdew, S. Burke, M. Ernzerhof, *Phys. Rev. Lett.* **77**, 3865 (1996).
- [12] D. Vanderbilt, *Phys. Rev. B* **41**, 7892 (1990).
- [13] H. J. Monksorst, J. D. Pack, *Phys. Rev. B* **13**, 5188 (1976).
- [14] P. E. Blochl, O. Jepsen, O. K. Andersen, *Phys. Rev. B* **49**, 16223 (1994).
- [15] A. E. Dwight, *Trans. Am. Soc. Met.* **53**, 479 (1961).
- [16] K. Sun, X. M. Guo, E. Wu, Y. T. Liu, H. L. Wang, *Physica B* **385-386**, 137 (2006).
- [17] X. M. Guo, Institute of Metal Research Chinese Academy of Sciences, Shenyang (2008).
- [18] N. I. Medvedeva, Y. N. Gornostyrev, D. L. Novikov, O. N. Mryasov, A. J. Freeman, *Acta Mater.* **46**, 3433 (1998).
- [19] B. R. Sahu, *Mater. Sci. Eng. B* **49**, 74 (1997).
- [20] H. Nakamura, D. Nguyen-Manh, D. G. Pettifor, *J. Alloys Compd.* **281**, 81 (1998).
- [21] S. V. Meschel, O. J. Kleppa, *J. Alloys Compd.* **415**, 143 (2006).
- [22] A. L. Shilov, M. E. Kost, N. T. Kuznetsov, *J. Less-Common Met.* **105**, 221 (1985).
- [23] R. Griessen, A. Driessen, D. G. De Groot, *J. Less-Common Met.* **103**, 235 (1984).
- [24] V. I. Zubov, N. P. Tretyakov, J. N. Teixeira Rabelo, J. F. Sanchezortiz, *Phys. Lett. A* **198**, 470 (1995).
- [25] M. M. Wu, B. T. Tang, L. M. Peng, W. J. Ding, *Phys. B* **405**, 4812 (2010).
- [26] K. Yukawa, K. Nakatsuka, M. Morinaga, *Sol. Energ. Mat. Sol. C.* **62**, 75 (2000).
- [27] P. V. Jasen, E. A. González, G. Brizuela, O. A. Nagel, G. A. González, A. Juan, *Int. J. Hydrogen Energy* **32**, 4943 (2007).
- [28] J. S. Kima, S. Y. Oh, G. Lee, Y. M. Koo, S. E. Kulkova, V. E. Egorushkin, *Int. J. Hydrogen Energy* **29**, 87 (2004).

*Corresponding author: du511@163.com